SURGICAL TECHNIQUE

Real-time navigation for liver surgery using projection mapping with indocyanine green fluorescence: development of the novel Medical Imaging Projection System.

Hiroto Nishino, MD[1], Etsuro Hatano, MD, PhD[1,2], Satoru Seo, MD, PhD[1], Takashi Nitta, MD, PhD[1,3], Tomoyuki Saito[4], Masaaki Nakamura[4], Kayo Hattori[5], Muneo Takatani, PhD[5], Hiroaki Fuji, MD[1], Kojiro Taura, MD, PhD[1], Shinji Uemoto, MD, PhD[1]

1 Department of Surgery, Graduate School of Medicine, Kyoto University, Kyoto, Japan

2 Department of Surgery, Hyogo College of Medicine, Hyogo, Japan

3 Department of Surgery, Mitsubishi Kyoto Hospital, Kyoto, Japan

4 Panasonic AVC Networks Company, Osaka, Japan

5 Institute for Advancement of Clinical and Translational Science, Kyoto University Hospital, Kyoto, Japan

Corresponding Author: Etsuro Hatano, MD, PhD

Department of Surgery, Hyogo College of Medicine

1-1 Mukogawa-cho, Nishinomiya, Hyogo 663-8501, Japan

Telephone number: +81-798-45-6582

Fax number: +81-798-45-6581

E-mail: shatano@hyo-med.ac.jp

Keywords

Liver; navigation surgery; fluorescence; indocyanine green; projection mapping

Requests for reprints: Reprints will not be available from the authors.

Sources of support for the work: This study was funded by the Translational Research Network Program of the Japan Agency for Medical Research and Development and the Acceleration Transformative research for Medical innovation of the Japan Agency for Medical Research and Development.

Conflicts of Interest and Source of Funding: There are no conflicts of interest.

A short running head: Real-time navigation for liver surgery

Mini-Abstract

We present a new imaging device, the Medical Imaging Projection System (MIPS), which uses the indocyanine green emission signal and active projection mapping. Our retrospective analysis suggests the potential feasibility and clinical utility of the MIPS to provide real-time navigation for liver resection.

Structured Abstract

Objective: The aim of this study was to evaluate the usefulness of a new imaging device, the Medical Imaging Projection System (MIPS), which uses the indocyanine green (ICG) emission signal and active projection mapping, for liver resection.

Summary Background Data: During anatomic liver resection, surgeons cannot completely view the intraparenchymal structure. Although a fluorescent imaging technique using ICG has recently been developed for hepatobiliary surgery, limitations in its application for real-time navigation persist.

Methods: We conducted a retrospective review of surgical and clinical outcomes for 23 patients who underwent anatomic hepatectomy using the MIPS and 29 patients who underwent the procedure without MIPS guidance, between September 2014 and September 2015.

Results: Preoperative characteristics were comparable between the two groups. No significant between-group differences were identified with regard to surgical and clinical outcomes. The demarcation lines were clearly projected by the MIPS in 21 patients; however, the boundary line was undetectable in 2 patients.

Conclusions: We developed the MIPS to address limitations in current intraoperative imaging methods. Our retrospective analysis provides evidence of the feasibility and clinical utility of the MIPS to identify anatomical landmarks for parenchymal dissection. The MIPS holds promise as a novel real-time navigation system for liver resection.

INTRODUCTION

Liver resection is the mainstay curative treatment for liver tumors,[1,2] with anatomic hepatectomy recommended for the treatment of hepatocellular carcinoma and some metastatic liver cancers.[3] As surgeons cannot completely view the intra-parenchymal structure, only the hepatic veins are available as landmarks to perform liver parenchymal dissection in many cases.

Recently, a fluorescent indocyanine green (ICG) based imaging technique has been developed to safely provide an anatomical view of the liver parenchyma for hepatobiliary surgery.[4] However, this imaging technique requires surgeons to use a handheld camera to capture the images, with Image quality affected by hand movement and physiological tremor. The technique also requires dimming of light within the operative field to prevent white light contamination of images. Moreover, the fluorescent images are displayed on a monitor, which requires that surgeons shift their field of vision to and from the images and real organs under a darkened operative field. Making incisions under such conditions is highly stressful.

To address these issues, we present a new imaging device, the Medical Imaging Projection System (MIPS), which uses the ICG emission signal and active projection mapping. The MIPS allows surgeons to determine the accurate cutting plane and the proper dissecting direction during anatomic hepatectomy, which, therefore, could provide an option for real-time navigation for liver surgery.

METHODS

Patients

Between September 2014 and September 2015, 52 patients underwent anatomic hepatectomy at the Kyoto University Hospital. We obtained consent from all patients to use the MIPS, regardless of the cancer type and surgical procedure, as long as the device was available. Ultimately, 23 anatomic hepatectomy procedures were performed under MIPS-guidance and 29 case without. We conducted a retrospective analysis of the medical records to compare outcomes between patients who underwent hepatectomy *with* and *without* MIPS. Our study protocol was approved by the ethics committee of the Graduate School of Medicine, Kyoto University (approval code: C857 and R955). The study was registered with the University Hospital Medical Information Network (unique trial number: UMIN000014998).

Preoperative evaluation of surgical operations

Three-dimensional (3D) images of the liver were created using SYNAPS VINCENT software (Fujifilm Medical Co., Ltd., Tokyo, Japan), based on preoperative computed tomography (CT) images. The remnant parenchymal volume ratio after removal of cancer-bearing segments was estimated from the 3D reconstructed images. We proceeded with anatomic hepatectomy for the treatment of liver tumors when the ratio of the remnant liver volume to the total liver volume met

our criterion for resection. Our criterion is determined using the preoperative indocyanine green Krem index (ICGK-rem), calculated by multiplying the ICG disappearance rate with the ratio of the remnant liver volume to the total liver volume.[5] The surgical procedure was determined based on the Liver Resection Guidelines of the International Hepato-Pancreato-Biliary Association.[6]

Administration of ICG

To provide a fluorescent source, 0.25 mg of ICG (2.5 mg/mL Diagnogreen; Daiichi Sankyo Co., Tokyo, Japan) was injected either intravenously after clamping the Glissonian sheaths flowing in the cancer-bearing hepatic segment, or directly into the portal branches supplying blood flow to the tumor-bearing hepatic segment, after puncturing of the target segments under intraoperative ultrasonography guidance. ICG was administered just before parenchymal dissection, but after liver mobilization and necessary taping of the Glissonian sheath.

Fluorescent imaging system

The MIPS was developed in collaboration with the Panasonic AVC Networks Company (Osaka, Japan) and includes a projection head and a pole (Fig.1A). The projection head uses a half mirror to match the optical axis of the camera and the projector, and is used during the procedure to obtain the location of the dye and to adjust image projection for guidance in real-time, regardless of shifting and deformation of the organ. The difference between a location on the real organ and the projected

image is within 1 mm, with the time lag between the fluorescent ICG emission in the liver and the projected image being within 100 ms. The projection head is designed to be located about 100 cm above the operative field, and not held by the surgeon (Fig. 1B). Detection thresholds for the MIPS can be selected based on the multi-step mode of fluorescent intensity (heat maps) or be manually selected. Moreover, the optical design, combining a half mirror and optical filter, selectively detects the ICG emission, with the MIPS removing white-light interference from the projected images. The algorithm subsequently converts both fluorescent-emitting and non-emitting tissues into specific colors and white, respectively, thereby differentiating projected from non-projected areas of the target region. This differentiation allows for a well-lit operative field without requiring use of a shadowless lamp (Fig.1C). The system is also customizable, allowing surgeons to select a preferred color to identify the real organ tissue. The set-up of the MIPS within the operative field requires only a few minutes. The operative field using the MIPS is shown in Supplementary Digital Content 1. A patent for this system has been obtained from the Japan Patent Office (unique number: PCT/JP2015/004946). This device has not yet been approved by the FDA and is still investigational.

CLINICAL ANALYSIS

We evaluated the feasibility and safety of using the MIPS by conducting a retrospective analysis of the perioperative characteristics and of the operative and postoperative outcomes of patients who

underwent anatomic hepatectomy *with* and *without* using the MIPS system (MIPS group and non-MIPS group, respectively). For analysis, clearly projected demarcation lines on MIPS images corresponded, morphologically, to lines observable on the preoperative 3D images.

STATISTICAL ANALYSIS

All statistical analyses were performed using SAS software (JMP 12.0.1; SAS Institute Inc., Cary, NC). Continuous variables were expressed as mean values±standard deviation and compared using Student's *t*-test between MIPS and non-MIPS group. Between-group differences on categorical variables were evaluated using chi-squared or Fisher exact tests as appropriate for the dataset. Survival rates were calculated using the Kaplan-Meier method and the log-rank test. P-value < 0.05 were considered to be significant.

RESULTS

Preoperative characteristics are summarized in Table 1, with no significant between-group differences identified except for the type and stage of cancer progression. Operative time and volume of blood loss was comparable between the groups. The demarcation lines were clearly projected by the MIPS in 21 patients, but were undetectable in 2 patients. Although parenchymal transection was performed by tracing the projected MIPS image in only 5 cases, the correspondence between the MIPS-detected boundary lines of deep liver parenchyma to those

identified on preoperative 3D images was confirmed in the cases. Postoperatively, the rate of morbidity was comparable between the two groups. However, the one-year disease free survival rate was higher among patients in the MIPS group than in the non-MIPS group, although this difference was not statistically significant.

Three exemplar case reports are presented, with specific patient characteristics summarized in Supplementary Data Content 2.

Patient 1

The largest tumor was identified in hepatic segment IV on preoperative CT (Fig. 2A). Based on the reconstructed preoperative 3D images (Fig. 2B), an extended left hepatectomy and partial liver resection of segment VIII were planned. Intraoperatively, the branch of the left Glissonian sheath was taped and the blood flow was blocked by clamping the sheath. The demarcation line of the ischemic region was identified by direct vision (Fig. 2C). ICG was injected intravenously and fluorescent images obtained, using the conventional system (Fig. 2D), and projected onto the surface of the liver using the MIPS (Fig. 2E; Supplementary Digital Content 3). The dissection line to secure the margin of the mass in segment IV was determined based on preoperative imaging and intraoperative ultrasonography. The cutting line crossed the colored area and the both cutting surface was colored due to the extended left hepatectomy and partial resection of segment VIII required (Fig. 2F).

Patient 2

The preoperative CT localized a tumor in hepatic segment V (Fig. 3A). Based on the reconstructed preoperative 3D images (Fig. 3B), an anatomic right anterior sectionectomy was planned. Intraoperatively, the tumor was exposed on the surface of hepatic segment V and the tumor-occupied area was projected using the MIPS (Fig. 3C). Injection of ICG was not required due to the persisting ICG around the tumor from the preoperative test. One of the anterior branches of the portal vein was identified by ultrasonography and the sheath was punctured using a 23-gauge needle for intra-portal ICG injection. Fluorescent images were obtained, using the conventional system (Fig. 3D), and projected onto the liver surface by the MIPS (Fig. 3E; Supplementary Digital Content 4). Fluorescent images included the exposed tumor area and the area of involvement identified by the ICG signal. The dissection line was determined based on reference images from the hepatic segment VIII and the preoperative 3D images of hepatic segment V, with the boundary between the colored and non-colored area in segment VIII corresponding to the cutting line on the preoperative 3D images (Fig. 3F). For treatment, a right anterior sectionectomy was performed.

Patient 3

Preoperative CT images identified a tumor located in hepatic segment VII (Fig. 4A). Based on the reconstructed preoperative 3D images (Fig. 4B), an anatomic right posterior sectionectomy was

planned. Intraoperatively, the branch of the right posterior Glissonian sheath was taped and blood flow was blocked by clamping the sheath. The demarcation line on the liver surface was barely recognizable (Fig. 4C), particularly on the gallbladder bed (Fig. 4D). ICG was injected intravenously and fluorescent images obtained using the conventional system (Fig. 4E) and projected onto the liver surface using the MIPS. The projected image smoothly followed the movement and deformation of the liver, and a right posterior sectionectomy was performed by tracing the projected MIPS image during parenchymal dissection (Fig. 4F; Supplementary Digital Content 5).

DISCUSSION

Liver resection offers the greatest potential for curative treatment for patients with liver cancer, with liver transplantation and radiofrequency ablation providing additional options depending on tumor size, location and stage of disease progression.[1,7] However, even experienced surgeons must manage significant technical difficulties during hepatectomy, with a slight error carrying the risk for serious complications, including massive bleeding and hepatic failure. The Japanese national clinical database system reported a 4.0% risk of hepatectomy-related mortality.[8]

Anatomic resection of the cancer-bearing portal territories is a reasonable procedure for the treatment of hepatocellular carcinoma, as well as for some patients with metastatic liver cancer.[3,9] This procedure requires precise identification of the intersegmental plane, which is not always flat.[10]

Two approaches are generally used to identify the demarcation line of the tumor area. The first approach involves surgical puncture of the portal branches supplying the cancer-bearing hepatic segments, under intraoperative ultrasonography guidance, with confirmation of the hepatic surface by injecting indigo-carmine or methylene blue stain.[11,12] Although indigo-carmine enhances the detectability of hepatic segments as a landmark for parenchymal dissection, its effectiveness is limited overall.[13] In the second approach, surgeons isolate and tape the Glissonian sheaths flowing in the cancer-bearing hepatic segment, followed by clamping of the sheaths to block blood flow with subsequent determination of the demarcation line of ischemic regions on the liver surface.[3,14] Surgeons can then determine the cutting line based on the demarcation line and location of the main hepatic veins. However, the demarcation line is unidentifiable under direct vision because of cirrhosis or severe adhesions.[13,15]

Although 3D simulated imaging of the liver, based on preoperative CT images, has progressed over the years,[16-18] the liver can move freely and change its shape during surgery, making precise identification of the internal anatomy of the tumor sites or vessels difficult based on static images. More recently, 3D printing has been used to create a see-through model of the liver, which can be used as a reference within the operative field.[19,20] However, this static approach still does not account for intraoperative movement or deformation of the liver.

Surgical molecular navigation, using fluorescent-labeled markers to identify tumor tissue using contrasting pseudocolors, has been developed.[21] In particular, fluorescent imaging using ICG and

a near infrared camera system has been adopted worldwide, with supporting research.[4] As the excitation spectrum and the peak wavelength of the ICG emission signal lies within the range of absorbance of hemoglobin and water,[22,23] ICG-imaging can detect small liver tumors and the bile duct.[24,25] Moreover, fluorescent imaging obtained by injecting ICG into the portal branch or peripheral vein can be used for intraoperative identification of hepatic segments.[26,27] The MIPS extends the ICG technique, combining ICG-emission imaging with active projection mapping, without requirement for use of special goggles or computer screens. The MIPS is superior to conventional imaging systems, as follows: surgeons can concentrate on the surgical field without having to shift their vision to other components for visualization of the area of interest; the image quality is not influenced by movement contamination of hand-held imaging devices; the necessity to darken the operative field to avoid white light contamination is eliminated; and accurate real-time projection makes it possible to follow the movement and deformation of the liver to maintain accuracy.

In Patient 1, ICG was distributed into the preserving area and the demarcation line was clearly projected (Fig. 2E), and corresponded to the boundary identified under direct visualization after clamping the left Glissonian sheath (Fig. 2C). In Patient 2, ICG was distributed more diffusely within the target area for resection, with difficulty in effectively puncturing the smaller branches of the portal vein, identified on preoperative 3D images as providing the main blood supply to hepatic segment V. In this case, we identified the demarcation line using both the MIPS image projected

on the liver and the reference, preoperative 3D images of hepatic segment V. In Patient 3, the MIPS-projected boundary was more clearly visible than the demarcation line identified by direct visualization, particularly on the gallbladder bed, with the anatomic right posterior sectionectomy performed by tracing the projected fluorescent image which differentiated hepatic segments (Fig. 4E). As the MIPS image is projected directly on the cutting surface, the dissection line, corresponding to the boundary between colored and non-colored areas, corresponded to the intersegmental plane, and was consistent even in the deep regions of the liver. Although the MIPS was used in only a few of our cases for parenchymal transection in the deep part of the liver, we found the MIPS imaging in these cases very useful. The colored plane can also be used to identify errors of extending the cutting line into non-ischemic tissue. Transecting the liver parenchyma along entire MIPS boundary would allow surgeons to accomplish the anatomic hepatectomy, as the cutting line is identified using appropriate timing and route of injection of the fluorescent ICG following portal vein ligation.

The demarcation line could not be identified using the MIPS in 2 cases. In one case, this was due to the misidentification of the cancer-bearing Glissonian sheath under intraoperative ultrasonography guidance, which requires expertise. In the other case, the demarcation line could not be detected because the procedure involved ligation of the Glissonian sheath originating in the branch of the left Glissonian sheath. Patients for whom surgeons can isolate the Glissonian sheaths flowing into the cancer-bearing hepatic segment are more suitable for MIPS use.

From our experience, the image thresholding mode was effective in correcting for the effects of a shorter staining time and lower ICG concentration for intravenous, rather than intra-portal, ICG injection.[27] Setting of a high detection sensitivity permitted detection of the demarcation line in patients with liver cirrhosis in whom the line was unclear under white light. In fact, the MIPS demarcation line was clearly projected for the one patient with Child Pugh Score B liver cirrhosis. The ICGR15 and ICGK levels were within normal limits in the two cases in which the MIPS did not project a clear demarcation line and subsequent investigation is required to clarify effects of the Child Pugh score on the anatomic visibility provided by the MIPS.

The principal clinical benefit of the MIPS is the continuous projection it provides to guide transection in the deep part of liver parenchyma, which is not possible with the conventional imaging technique, due to shifting of visual focus, image blurring due to hand-shaking, and low visibility due to the required darkening of the operative field. Moreover, real-time MIPS navigation corrects for movement and deformation of the organ during surgery to secure consistent accuracy of the projected image. The development of reliable and accurate real-time navigation systems, such as the MIPS, is important, particularly in view of recent increases in the use of laparoscopy for liver resection. New devices, which integrate ICG images with laparoscopic system[28,29] have great potential to be widely accepted in the near future. Based on our experience, we propose that the MIPS should be used even when other techniques are available, including 3D simulation imaging of the liver based on preoperative CT and intraoperative ultrasonography. Non-clearance of ICG

injected preoperatively to assess liver function around the tumor may cause confusion of the correct projection line, as in patient 2 in our case series. Attention is also needed in cases in which the tumor lies close to the cutting line, requiring the use of 3D simulation based on preoperative CT imaging and intraoperative ultrasonography. 5-aminolevulinic acid (5-ALA), a fluorescence material recently used for detection of liver tumors,[30] and ICG used in a double-tracer technique might further enhance the boundary between the tumor and the cutting line.

In conclusion, the MIPS provided reliable identification of landmarks for the parenchymal dissection by combining active projection mapping to fluorescence-guided imaging. Further research is needed to fully determine if the resection plane projected by the MIPS is sufficiently precise for a real-time navigation. A clinical trial comparing the accuracy of parenchymal transection between MIPS guided hepatectomy and conventional hepatectomy is currently in progress.

ACKNOWLEDGEMENTS

This study was supported by the Translational Research Network Program of the Japan Agency for Medical Research and Development and the Acceleration Transformative research for Medical innovation of the Japan Agency for Medical Research and Development.

REFERENCES

1. Benson AB 3rd, Abrams TA, Ben-Josef E, et al. NCCN clinical practice guidelines in oncology: hepatobiliary cancers. *J Natl Compr Canc Netw.* 2009;7:350-391.

2. Benson AB 3rd, Bekaii-Saab T, Chan E, et al. Metastatic colon cancer, version 3.2013: featured updates to the NCCN Guidelines. *J Natl Compr Canc Netw.* 2013;11:141-152.

3. Hasegawa K, Kokudo N, Imamura H, et al. Prognostic Impact of anatomic resection for hepatocellular carcinoma. *Ann Surg.* 2005;242:252-259.

4. Ishizawa T, Kokudo N. The beginning of a new era of digestive surgery guided by fluorescence imaging. *Liver Cancer.* 2014;3:6-8.

5. Takasaki T, Kobayashi S, Suzuki S, et al. Predetermining postoperative hepatic function for hepatectomies. *Int Surg.* 1980;65:309–313.

6. Belgihiti J, Clavien PA, Gadzijev, et al. The Brisbane 2000 terminology of liver anatomy and resections. *HPB.* 2000;2:333-339.

7. Torzilli G, Donadon M, Cimino M. Are Tumor Exposure and Anatomical Resection Antithetical during Surgery for Hepatocellular Carcinoma? A Critical Review. *Liver Cancer.* 2012;1:177-182.

8. Kenjo A, Miyata H, Gotoh M, et al. Risk stratification of 7,732 hepatectomy cases in 2011 from the National Clinical Database for Japan. *J Am Coll Surg.* 2014;218:412-422.

9. Regimbeau JM, Kianmanesh R, Farges O, et al. Extent of liver resection influences the outcome

in patients with cirrhosis and small hepatocellular carcinoma. *Surgery.* 2002;131:311-317.

10. Shindoh J, Mise Y, Satou S, et al. The intersegmental plane of the liver is not always flat--tricks for anatomical liver resection. *Ann Surg.* 2010;251:917-922.

11. Makuuchi M, Hasegawa H, Yamazaki S. Ultrasonically guided subsegmentectomy. *Surg Gynecol Obstet.* 1986;161:346-350.

12. Ahn KS, Kang KJ, Park TJ, et al. Benefit of systematic segmentectomy of the hepatocellular carcinoma: revisiting the dye injection method for various portal vein branches. *Ann Surg.* 2013;258:1014-1021.

13. Miyata A, Ishizawa T, Tani k, et al. Reappraisal of a dye-staining technique for anatomic hepatectomy by the concomitant use of indocyanine green fluorescence imaging. *J Am Coll Surg.* 2015;221:e27-e36.

14. Takasaki K. Glissonean pedicle transection method for hepatic resection: a new concept of liver segmentation. *J Hepatobiliary Pancreat Surg.* 1998;5:286-291.

15. Uchiyama K, Ueno M, Ozawa S, et al. Combined intraoperative use of contrast-enhanced ultrasonography imaging using a sonazoid and fluorescence navigation system with indocyanine green during anatomical hepatectomy. *Langenbecks Arch Surg.* 2011;396:1101-1107.

16. Saito S, Yamanaka J, Miura K, et al. A novel 3D hepatectomy simulation based on liver circulation: Application to liver resection and transplantation. *Hepatology.* 2005;41:1297-304.

17. Fang CH, Tao HS, Yang J, et al. Impact of three-dimensional reconstruction technique in the

operation planning of centrally located hepatocellular carcinoma. *J Am Coll Surg.* 2015;220:28-37.

18. Hallet J, Gayet B, Tsung A, et al. Systematic review of the use of pre-operative simulation and navigation for hepatectomy: current status and future perspectives. *J Hepatobiliary Pancreat Sci.* 2015;22:353-362.

19. Zein NN, Hanouneh IA, Bishop PD, et al. Three-dimensional print of a liver for preoperative planning in living donor liver transplantation. *Liver Transpl.* 2013;19:1304-1310.

20. Igami T, Nakamura Y, Hirose T, et al. Application of a Three-dimensional Print of a Liver in Hepatectomy for Small Tumors Invisible by Intraoperative Ultrasonography: Preliminary Experience. *World J Surg*. 2014;38:3163-3166.

21. Nguyen QT, Tsien RY. Fluorescence-guided surgery with live molecular navigation - a new cutting edge. *Nat Rev Cancer.* 2013;13:653-662

22. Landsman ML, Kwant G, Mook GA, et al. Light-absorbing properties, stability, and spectral stabilization of indocyanine green. *J Appl Physiol.* 1976;40:575-583.

23. Vahrmeijer AL, Hutteman M, van der Vorst JR, et al. Image-guided cancer surgery using near-infrared fluorescence. *Nat Rev Clin Oncol.* 2013;10:507-518.

24. Ishizawa T, Fukushima N, Shibahara J, et al. Real-time identification of liver cancers by using indocyanine green fluorescent imaging. *Cancer.* 2009;115:2491–2504.

25. Ishizawa T, Bandai Y, Ijichi M, et al. Fluorescent cholangiography illuminating the biliary tree during laparoscopic cholecystectomy. *Br J Surg.* 2010;97:1369-1377.

26. Aoki T, Yasuda D, Shimizu Y, et al. Image-guided liver mapping using fluorescence navigation system with indocyanine green for anatomical hepatic resection. *World J Surg.* 2008;32:1763-1767.

27. Inoue Y, Arita J, Sakamoto T, et al. Anatomical liver resections guided by 3-dimensional parenchymal staining using fusion indocyanine green fluorescence imaging. *Ann Surg.* 2015;262:105-111.

28. Ris F, Hompes R, Cunningham C, et al. Near-infrared (NIR) perfusion angiography in minimally invasive colorectal surgery. *Surg Endosc.* 2014;28:2221-2226.

29. Tanaka M, Inoue Y, Mise Y, et al. Laparoscopic deroofing for polycystic liver disease using laparoscopic fusion indocyanine green fluorescence imaging. *Surg Endosc.* 2016;30:2620-2623.

30. Inoue Y, Tanaka R, Komeda K, et al. Fluorescence detection of malignant liver tumors using 5-aminolevulinic acid-mediated photodynamic diagnosis: principles, technique, and clinical experience. *World J Surg.* 2014;38:1786-1794.

Legends for Figures

Fig. 1. The Medical Imaging Projection System (MIPS): a new fluorescent imaging device using projection mapping.

A. A pictorial view of the MIPS, showing the projection head and pole components.

B. The intra-operative view using the MIPS. The projection head (white bald arrow) is located about 100 cm above the operative field.

C. The operative field is well-lit without use of a shadowless lamp.

Fig. 2. An extended left hepatectomy performed for multiple liver metastases in a colon cancer patient using the Medical Imaging Projection System (MIPS) is shown.

A. Preoperative computed tomography (CT) revealed that the largest tumor (4 mm in diameter) to be located in hepatic segment IV (white bald arrow).

B. Preoperative three dimensional (3D) images based on CT imaging are shown. An extended left hepatectomy and partial liver resection of segment VIII was performed.

C. The demarcation line was identified by direct visualization of the ischemic region after clamping the branch of the left Glissonian sheath (between two black arrows).

D. The demarcation line was identified on the monitor with the conventional system after intravenous indocyanine green (ICG) injection (between two white arrowheads). The demarcation line is the same as the line presented in Fig. 2C.

E. The demarcation line was projected onto the surface of the liver with the MIPS after intravenous ICG injection (between two white arrows). The demarcation line is the same as the line presented in Fig. 2C and Fig.2D.

F. Projected MIPS images during parenchymal dissection of an extended left hepatectomy are shown, with the cutting line crossing the colored area to secure the margin of the mass in segment IV. The both cutting surface were colored.

Fig. 3. An anatomic right anterior sectionectomy for treatment of a hepatocellular carcinoma using the Medical Imaging Projection System (MIPS) is shown.

A. Preoperative computed tomography (CT) revealed that the tumor (30 mm in diameter) was located in hepatic segment V (white bald arrow).

B. Preoperative three dimensional (3D) images based on CT imaging are shown. An anatomic right anterior sectionectomy was performed.

C. The projected image using the MIPS before intraoperative indocyanine green (ICG) injection, showing the disordered biliary excretion of ICG in tumor by preoperative ICG test (white arrowhead).

D. The demarcation line was identified on the monitor with the conventional system after puncturing the target branch of portal vein and administering an intraportal ICG injection.

E. The demarcation line was projected onto the surface of the liver using the MIPS after puncturing target branch of portal vein and administering an intraportal ICG injection.

F. Projected MIPS image during parenchymal dissection in hepatic segment VIII of an anatomic right anterior sectionectomy are shown.

Fig 4. An anatomic right posterior sectionectomy for treatment of a hepatocellular carcinoma patient using the Medical Imaging Projection System (MIPS) is shown.

A. Preoperative computed tomography (CT) revealed that the tumor (30 mm in diameter) was located in hepatic segment VII (white bald arrow).

B. Preoperative three dimensional (3D) images based on CT imaging are shown. An anatomic right posterior sectionectomy was performed.

C. The demarcation line was not clearly identified by direct vision for the ischemic region after clamping the branch of the right posterior Glissonian sheath (between two white arrowheads).

D. The demarcation line on the gallbladder bed was not identified by direct vision for the ischemic region after clamping the branch of the right posterior Glissonian sheath.

E. The demarcation line was identified on the monitor with the conventional system after intravenous indocyanine green (ICG) injection (between two white arrows).

F. Results of the parenchymal dissection during an anatomic right posterior sectionectomy using the MIPS are shown. The projected area of the resected liver during parenchymal dissection should have been preserved. The dissection line was thought to be the boundary between the colored and non-colored area (between two black arrows).

Supplementary Digital Content 1.mp4

The operative field using the Medical Imaging Projection System (MIPS) is shown.

Supplementary Digital Content 2.doc

Characteristics of three cases using the Medical Imaging Projection System (MIPS) described in the manuscript.

Supplementary Digital Content 3.mp4

Intraoperative image projected onto the liver surface using the Medical Imaging Projection System (MIPS) after clamping the branch of the left Glissonian sheath and intravenous injection of indocyanine green (ICG) is shown.

Supplementary Digital Content 4.mp4

Intraoperative image projected onto the liver surface using the Medical Imaging Projection System (MIPS) after puncturing of the target branch of portal vein and administering an intraportal indocyanine green (ICG) injection is shown.

Supplementary Digital Content 5.mp4

Intraoperative image projected onto the liver surface using the Medical Imaging Projection System (MIPS) after clamping the branch of the right posterior Glissonian sheath and intravenous indocyanine green (ICG) injection is shown.

Table 1. Liver resection outcomes between patients who underwent anatomic hepatectomy *with* and *without* using the Medical Imaging Projection System (MIPS) system.

Variables	MIPS (n=23)	non-MIPS (n=29)	p
Preoperative characteristics			
Age years median (range)	66.9±10.7 (39-82)	65.1±11.8 (33-82)	0.57
Sex male: female	19:4	17:12	0.058
Previous liver resection n (%)	4 (17.4%)	5 (17.2%)	0.99
ICGR15 (range)	13.3±5.8 (5-26)	13.1±7.7 (4-30)	0.89
ICGK (range)	0.153±0.031 (0.087-0.215)	0.155±0.048 (0.067-0.254)	0.90
Child Pugh Score A:B:C	22:1:0	27:2:0	0.69
Hepatitis virus HBV:HCV:nonHBVnonHCV	4:4:15	4:8:17	0.67
Operative outcomes			
Surgical Procedure			
Left trisectionectomy n (%)	1 (4.3%)	-	
Right hepatectomy n (%)	8 (34.8%)	6 (20.7%)	
Central bisectionectomy n (%)	2 (8.7%)	1 (3.4%)	
Left hepatectomy n (%)	1 (4.3%)	6 (20.7%)	
Extended left hepatectomy n (%)	1 (4.3%)	2 (6.9%)	
Right posterior sectionectomy n (%)	3 (13.0%)	1 (3.4%)	
Extended right posterior sectionectomy n (%)	1 (4.3%)	-	
Right anterior sectionectomy n (%)	1 (4.3%)	1 (3.4%)	
Left medial sectionectomy n (%)	1 (4.3%)	2 (6.9%)	
Segmentectomy n (%)	4 (17.4%)	10 (34.5%)	
Operative time min (range)	483.1±152.5 (265-925)	483.7±195.5 (259-976)	0.99
Volume of blood loss ml (range)	1025.5±987.9 (62-4041)	1062.3±1434.9 (47-6350)	0.91
Blood perfusion n (%)	5 (21.7%)	9 (31.0%)	0.45
Lymphadenectomy n (%)	2 (8.7%)	5 (17.2%)	0.36
Vascular reconstruction n (%)	3 (13.0%)	1 (3.4%)	0.19
Biliary reconstruction n (%)	2 (8.7%)	3 (10.3%)	0.84
Clearly demarcation line on MIPS images n (%)	21 (91.3%)	-	
Postoperative outcomes			
Morbidity			
≧Grade 3 (Clavien-Dindo Classification) n (%)	4 (17.4%)	4 (13.8%)	0.72

Thoracoabdominal fluid retention n	2	2	
Bile leakage n	1	2	
Intraabdominal abscess n	1	2	
PHLF (ISGLS definition) n (%)	6 (26.1%)	9 (31.0%)	0.70
Grade A n	2	3	
Grade B n	3	5	
Grade C n	1	1	
Pathological findings			
Hepatocellular carcinoma n (%)	13 (56.5%)	19 (65.5%)	
Metastasis of colorectal cancer n (%)	8 (34.8%)	7 (24.1%)	
Cholangiocarcinoma n (%)	1 (4.3%)	2 (6.9%)	
Intraductal papillary neoplasm of bile duct n (%)	1 (4.3%)	1 (3.4%)	
Long-term outcomes			
1-year disease free survival rate (%)	75.4%	59.6%	0.21
1-year overall survival rate (%)	95.7%	96.2%	0.73

ICG, indocyanine green; ICGR15, indocyanine green retention rate at 15 minutes; ICGK, indocyanine green K index; MIPS, medical imaging projection system; HBV, hepatitis B virus; HCV, hepatitis C virus; PHLF, posthepatectomy liver failure; ISGLS, International Study Group of Liver Surgery

Fig. 1

A

B

C

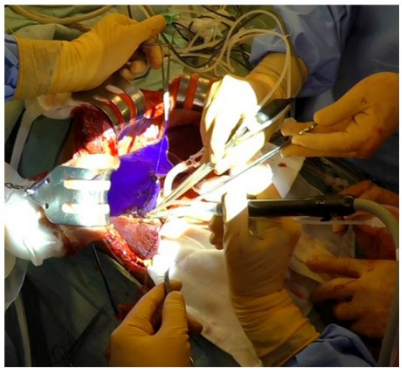

Fig. 2

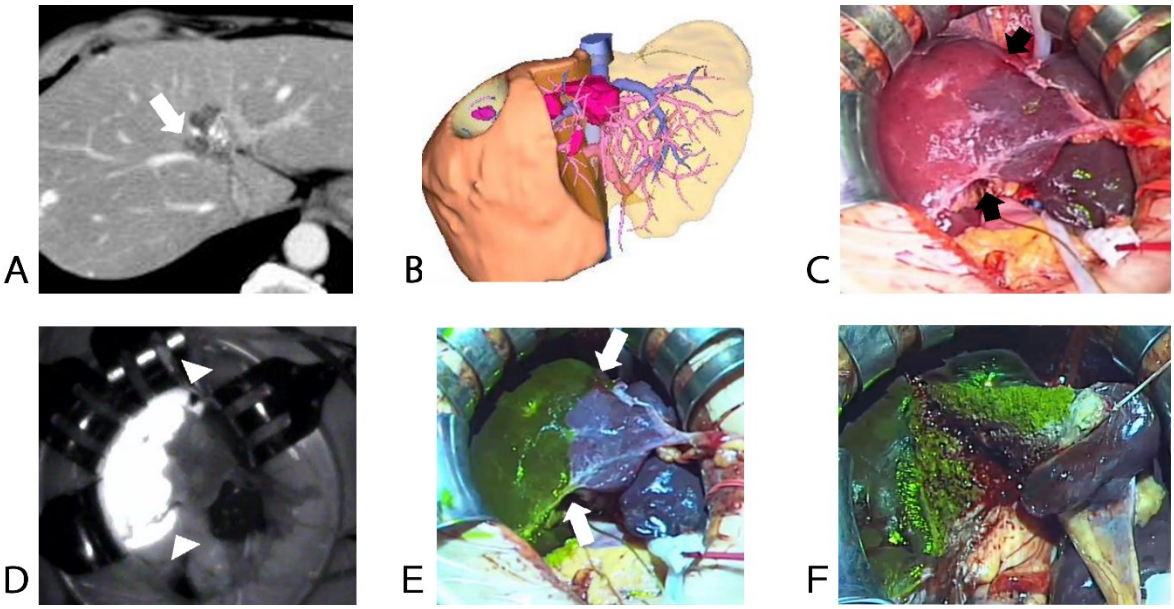

Fig. 3

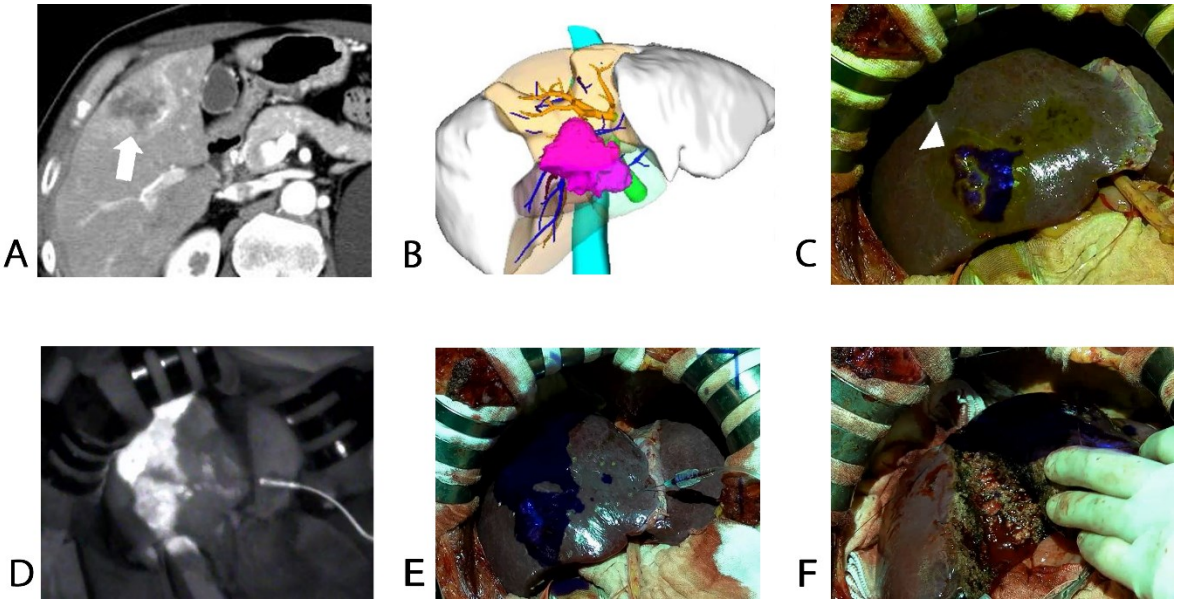

Fig. 4

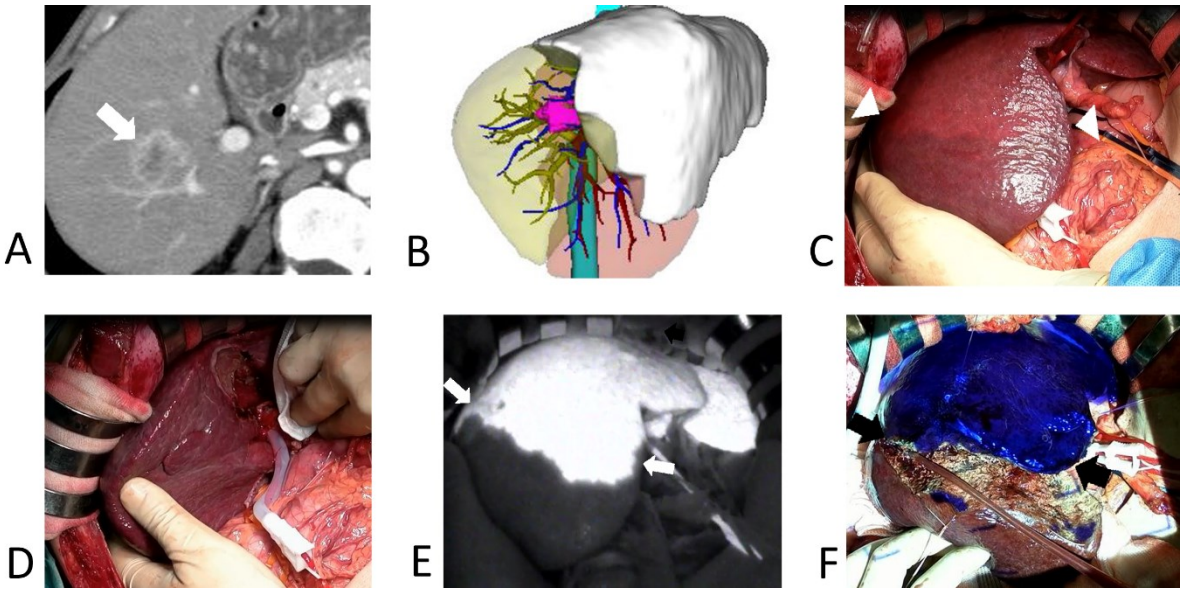

This is a non-final version of an article published in final form in https://doi.org/10.1097/SLA.0000000000002172.